Proc. Natl. Acad. Sci. USA
Vol. 86, pp. 6959–6962, September 1989
Biophysics

Photogating of ionic currents across a lipid bilayer

(porphyrin/photochemistry/electrostatics/lipophylic ions/membrane)

C. M. DRAIN, B. CHRISTENSEN*, AND D. MAUZERALL†

The Rockefeller University, 1230 York Avenue, New York, NY 10021

Communicated by George Feher, June 8, 1989 (received for review March 6, 1989)

ABSTRACT **Photoformation of metalloporphyrin cations in a lipid bilayer increases the ionic currents of negative and decreases those of positive hydrophobic ions. At low concentrations of the mobile hydrophobic ion, a 30% change in conductivity is observed that decreases with increasing concentration of positive tetraphenylphosphonium ion and increases drastically with increasing concentration of negative tetraphenylboride ion. In the region of saturated conductance of boride ion, the increase in conductivity is 3.6-fold. A 15-fold increase is observed with the protonophore carbonyl cyanide 3-chlorophenylhydrazone. In this case the net charge gated is 300 times greater than the photogenerated charge in the bilayer membrane. Thus there is a net gain in this organic field effect phototransistor. The gating can also be accomplished by continuous light or chemical oxidants. Photogating is explained as space charge effects inside the bilayer.**

There is great interest in the movement of ions across cell membranes since these currents are associated with the activity of all metabolically functional cells. In addition, there is much work aimed at understanding the chemical properties of these membranes (1). The planar lipid bilayer membrane as developed by Mueller *et al.* (2) has proven to be remarkably useful as a model of the cell membrane. It was discovered that small ions cross these membranes by two mechanisms: ion channels that can be gated by voltage or receptors (3, 4) and ion carriers that are not gated (5). We now show that the latter ionic currents, exemplified by currents of large hydrophobic ions, can be gated by photoinduced charge generation inside the membrane. The photogating effect is explained by local electrostatic effects in the bilayer membrane. The pigment/bilayer/hydrophobic ion system is an example of an organic field effect phototransistor (6).

Much work has been carried out on the mechanism by which ion carriers or hydrophobic ions cross the lipid bilayer (7–11). The large radius of these ionic species decreases the Born electrostatic charging energy of the ion, thus enabling them to traverse the hydrocarbon core of the membrane (10). It is striking that for hydrophobic ions of similar size, the conductivity of negative ions is 10^2–10^3 times that of positive ions (7, 8, 12, 13). This observation has been explained by a dipolar potential, originating in ordered ester carbonyl groups, which is positive toward the hydrocarbon core (12). Most studies of the kinetics of ion crossing monitor either current relaxations after an applied voltage step or voltage relaxations after a charge pulse (7, 9). These techniques, although very useful, are limited by capacitive transients and by ambiguity of interpretation (14). The present technique avoids the former problem and allows a direct measure of the transients in the change of conductivity.

The publication costs of this article were defrayed in part by page charge payment. This article must therefore be hereby marked "*advertisement*" in accordance with 18 U.S.C. §1734 solely to indicate this fact.

EXPERIMENTAL

The 4-ml plastic membrane cell was separated by a Teflon divider with a 1-mm^2 hole in the center and had glass slides for windows. A bilayer was formed from a solution of 3.2% (wt/vol) diphytanoylphosphatidylcholine in decane containing 3.6 mM magnesium octaethylporphyrin (MgOEP) across symmetrical solutions of 0.1 M NaCl, 10 mM Hepes (pH 7.1), and 20 mM methylviologen (acceptor). The light pulse was from a flash-pumped dye laser, 1 μs at 596 nm and 7 mJ maximum energy. The current was monitored by a pair of calomel electrodes with saturated KCl bridges immersed in the two solutions separated by the membrane. The current was measured with a fast operational amplifier with a feedback loop of adjustable gain and time constant and a variable series voltage source (0 to ±100 mv) on the input side, which polarizes the membrane. Typically, the operational amplifier was set at 10^7 V/A with a time constant of 0.1 s. The signal was digitized by means of a Keithley 194 high speed voltmeter or a Biomation 802 transient recorder and stored in a Hewlett–Packard 318 computer. Stock solutions of tetraphenylphosphonium ions ($TPhP^+$) and tetraphenylboride ions ($TPhB^-$) in ethanol/water, 1:1 (vol/vol), were added to each side of the membrane after it has formed. The counter ion for $TPhP^+$ is chloride and for $TPhB^-$ is sodium.

RESULTS

We have developed a method of photoinducing electron transfer across the lipid bilayer–water interface (15, 16) and have used this method to study the properties of this interface as well as the crucial polar region between the interface and the hydrocarbon core. A hydrophobic closed-shell metalloporphyrin in the polar region of the lipid bilayer is the electron donor. The ionic electron accepter is restricted to the aqueous phase. This self-organizing design ensures separation of charge on photoexcitation. The technique has the following characteristics: (*i*) the charge transfer is vectorial and has a quantum yield of 0.1 (15, 16); (*ii*) the forward electron transfer is a purely dynamic photoreaction and can occur in less than 5 ns (17); (*iii*) the porphyrin cation in the bilayer requires >0.1 s to cross the bilayer (18); (*iv*) the lifetime of the porphyrin cation is several seconds but can be shortened to microseconds by addition of aqueous ionic electron donors (16); and (*v*) unlike pulsed voltage measurements, there are no capacitive transients in the photogating of ionic currents. The symmetrical generation of charge (Fig. 1*A*) changes the electrical potential within the bilayer but has no effect on the electrodes in the ionic solutions.

The current of $TPhP^+$ across a diphytanoylphosphatidylcholine/MgOEP/decane bilayer decreases ≈25% when illu-

Abbreviations: $TPhB^-$, tetraphenylboride ion; $TPhP^+$, tetraphenylphosphonium ion; MgOEP, magnesium octaethylporphyrin.

*Present address: Institute of Biophysics, University of Frankfurt, Frankfurt, F.R.G.
†To whom reprint requests should be addressed.

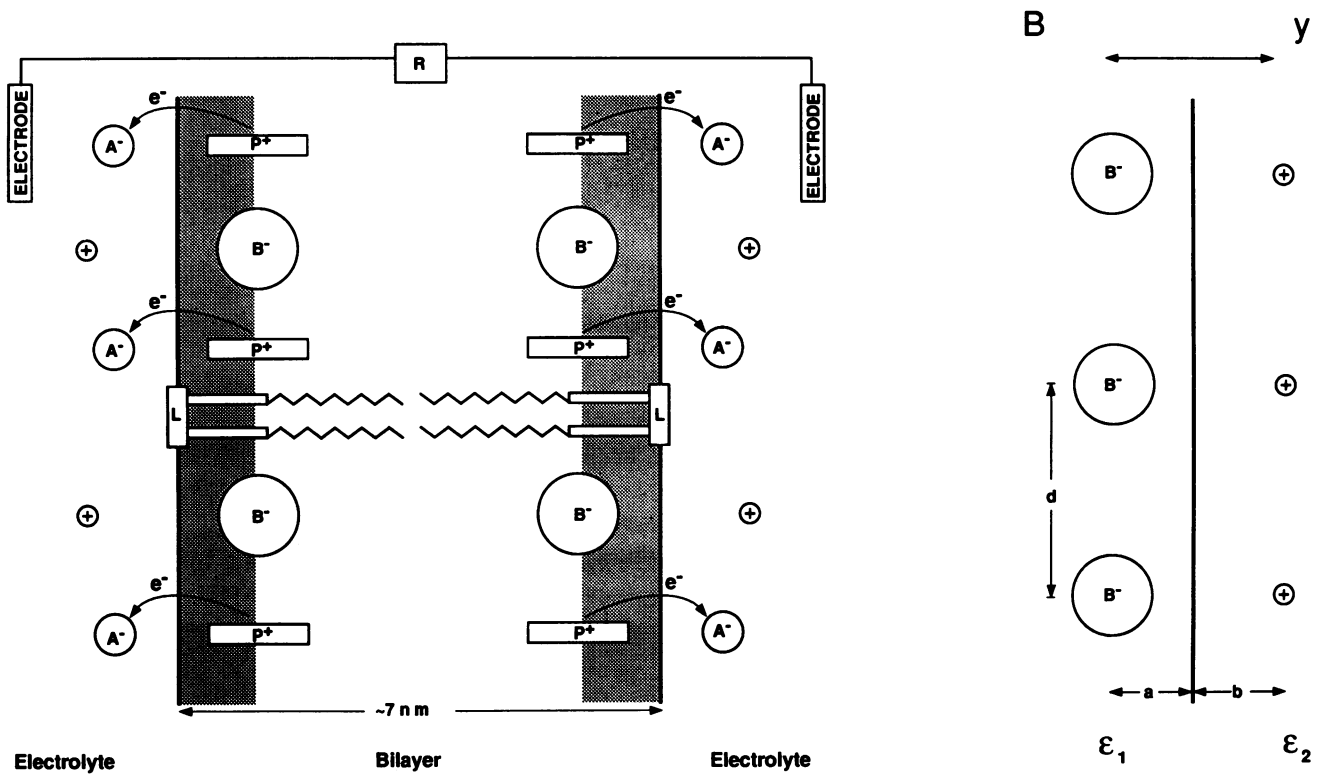

FIG. 1. (*A*) Schematic of the interfacial charge transfers and resulting positive charge within the bilayer. The lipids are labeled L, the hydrophobic porphyrin is P^+, the aqueous ionic electron accepter is A^-, the negative hydrophobic ion is B^-, and the aqueous counter ion is +. A voltage imposed across the electrodes allows the current to be recorded by R. Conductance is not limited by the aqueous ionic solution. The symmetrical charge separation guarantees no observable effect at the electrodes. The asymmetric situation occurs when the accepter is omitted from one side. A photovoltage is then observed by polarization of the nonreactive side. This photovoltage is independent of the applied voltage used in the experiments to measure current. The molecules are drawn roughly to scale but the lateral distance between the charges is much smaller (5–10 times) than in a typical experiment. (*B*) Schematic of electrostatic model used to calculate the energy of ions in the bilayer. Two-dimensional lattices of ionic charges are located in two dielectrics ($\varepsilon_1 < \varepsilon_2$) at depths of a and b from the interface. The distance d between the charges is much larger than what is shown. y is the axis perpendicular to the membrane.

minated by a 1-μs saturating flash of light at 596 nm (Fig. 2*A*). Fast kinetic transients in the current change after the flash, never observed with voltage or charge pulse methods, are readily measured. The current of $TPhB^-$, or of dipicrylamine, at low concentrations is in turn increased by about 50% upon similar illumination (Fig. 2*B*). However, at high concentrations of $TPhB^-$, where the dark conductance is saturated (7–9), dramatically larger increases of up to 360% in the current amplitude are observed upon illumination (Fig. 3*A*). The fast transient kinetics (not resolved in Fig. 2) are slowed by the space charge effects discussed below. Up to 15-fold increases in the current amplitude are seen with the protonophore carbonyl cyanide 3-chlorophenylhydrazone (Fig. 3*B*).

All four components—hydrophobic porphyrin, aqueous acceptor, hydrophobic ion, and a constant applied voltage—must be present to observe this effect. The cause of the conductance change is the presence of the porphyrin cation since increasing the concentration of an electron donor, which reduces the porphyrin cation, shortens the lifetime of the photoinduced current. The apparent second-order rate constant is comparable to that observed for the decay of the photovoltage in the asymmetric situation (15). Furthermore, the light-intensity dependence of the photogating amplitude follows that of porphyrin cation formation, as measured by the photovoltage in an asymmetrical experiment. The presence of hydrophobic ions does not cause an increased yield of porphyrin cations since they have no effect on the photovoltage in the asymmetric experiment. Photogating of lipophilic ion currents is also observed under pulsed continuous illumination. Chemical oxidation of MgOEP by dipotassium hexachloroiridate(IV) also causes the expected change in lipophilic ion currents across the membrane.

DISCUSSION

The photogating effect is ascribed to a change in potential sensed by the hydrophobic ions within the membrane. This inner potential determines both the equilibrium concentration of ions in the polar region and their conductance across the interfaces and the hydrocarbon core region. The hydrophobic ions partition into the polar region of the membrane and their charges generate a repulsive potential that limits the number of hydrophobic ions that can be absorbed into the membrane. The relation between the aqueous hydrophobic ion concentration (C) and the membrane concentration or volume charge density of absorbed ions (ρ_-) can be described by an implicit equation (19):

$$\rho_- = CKe^{-A\rho_-}, \quad [1]$$

where K is the partition coefficient that includes the hydrophobic and electrostatic energies of transferring the large ion from water to the polar region of the bilayer. The constant A is determined by the model used to estimate the electrostatic interactions in this heterogeneous system. For a two-dimensional lattice of hydrophobic ions at distance a from the membrane–water interface in dielectric ε_1 of the membrane and a corresponding lattice of counter ions at a distance b in the aqueous dielectric of ε_2 (Fig. 1*B*):

$$A = r_c Mg^2/\varepsilon_1, \quad [2]$$

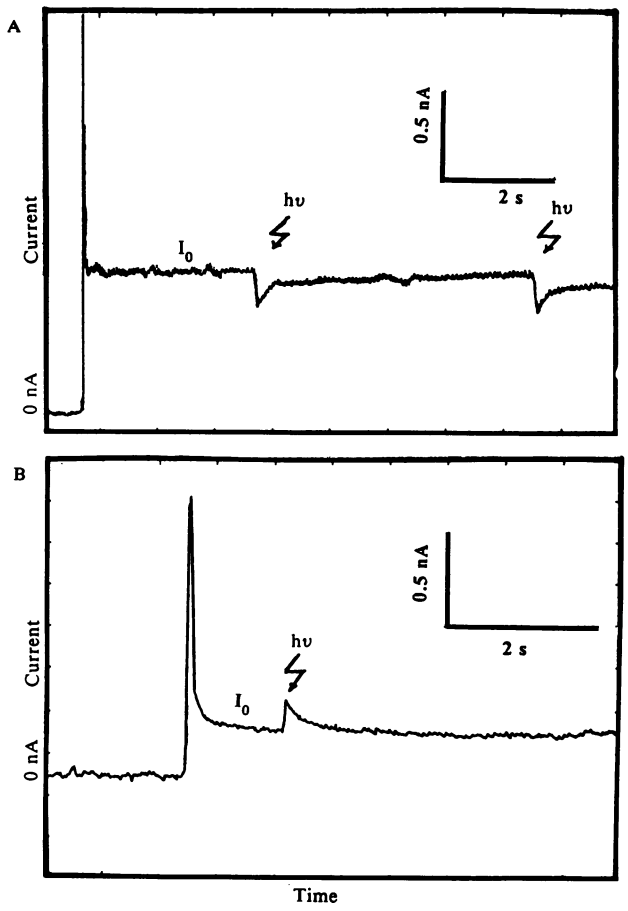

FIG. 2. (*A*) Current of 5 mM $TPhP^+$ decreases 25% on photocharging the lipid bilayer. (*B*) Current of 1 μM $TPhB^-$ through a planar lipid bilayer increases 50% upon photocharging the membrane. Light pulses are indicated by arrows. In each case the applied voltage is +50 mV. The spikes to the left of the photosignal are the relaxation currents after imposition of the voltage. The baseline current is indicated by I_0.

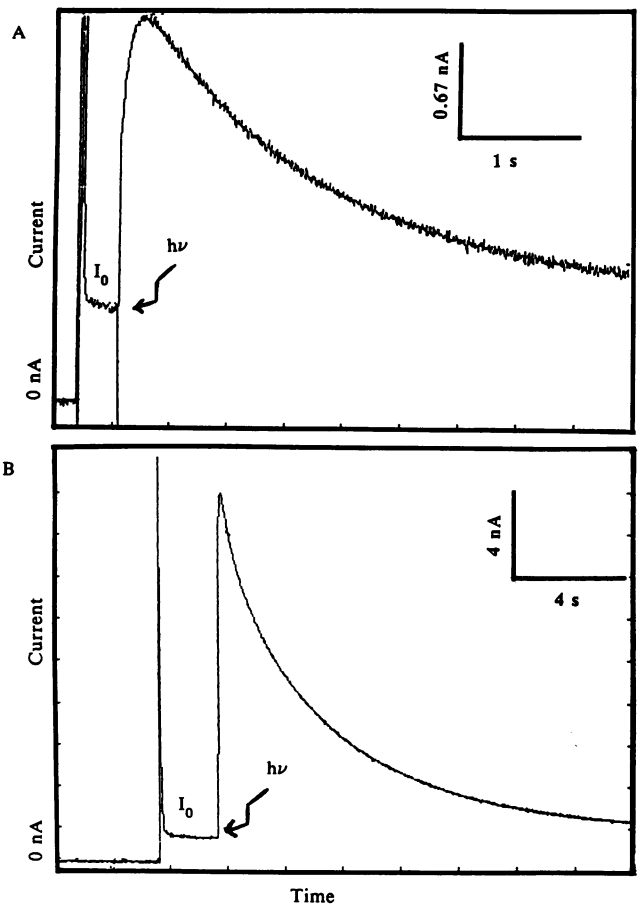

FIG. 3. (*A*) Large photogating effect in the regime of saturated conductance of $TPhB^-$. The photogated increase in current, ΔI, is 3 times the baseline current I_0. The concentration of $TPhB^-$ is 0.13 mM, and the applied voltage is +50 mV. The current scale factor should be multiplied by 10. (*B*) A 15-fold increase in current is observed when the protonophore carbonyl cyanide 3-chlorophenylhydrazone is the membrane-soluble ion. The concentration of carbonyl cyanide 3-chlorophenylhydrazone is 0.15 μM, with an applied voltage of +40 mV. As in Fig. 2, the relaxation currents are to the left of the photosignal.

where $r_c = e^2/4\pi\varepsilon_0 kT = 56$ nm and $g^2 = [2(\varepsilon_2 - \varepsilon_1)a^2 + \varepsilon_1(a + b)^2]/(\varepsilon_1 + \varepsilon_2)$; r_c is the Coulomb radius *in vacuo*, g^2 is the dielectric weighted distance squared, ε_0 is the vacuum permitivity, k is the Boltzmann constant, T is the temperature, and M is the Madelung constant for the infinite lattice. For a two-dimensional square lattice M is 9.03 (20). The derivation of Eq. **2** is based on the method of images in electrostatics (12, 13, 19, 21).

Eq. **1** can be solved numerically and the data on saturation of conductance at high concentrations of hydrophobic ions can be explained by the simple assumption that the conductivity is proportional to ρ_- not C. For the $TPhB^-$ the partition coefficient (22) is 10^5 and the cross core transfer of $TPhB^-$ decreases e-fold ($A\rho_- = 1$) at about 1 μM (19). At this concentration ρ_- is calculated from Eq. **1** to be 0.02 nm^{-3}. The depth a is estimated to be $\approx$1 nm (i.e., the polar region of the bilayer) because of the ion's hydrophobicity. The counter ion can be assumed to be located at the Debye length in the aqueous phase, 1 nm in 0.1 M NaCl. For this case, $a = b$, so $g^2 = 2a^2$. ε_1 is calculated from Eq. **2** to be 25, which is reasonable for the polar region of the membrane (19, 22–25). Because of the large size of the ions and the complex nature of the polar region, the distance a and the dielectric constant ε_1 must be understood as a suitable average over these parameters. Saturation of the conductivity occurs when the lattice spacing d is 7 nm, which is greater than the estimated ion depth ($a \approx 1$ nm), justifying the use of a two-dimensional lattice model. It is this limited dimensionality that produces the large Madelung constant. Thus the conductivity is limited by the space charge (8, 26, 27) and a clear theoretical discussion is presented by de Levie and co-workers (28–31).

The photogating effect can be explained by the photoinduced formation of a similar lattice of porphyrin cations of density ρ_{p+}. By superposition, the potential of this lattice will algebraically add to that of the hydrophobic ions and affect their concentration and conductance accordingly. The observed photogating effect at low hydrophobic ion concentration can be expressed as an energy of + or − 0.3 kT. An estimate of ρ_{p+} from the observed photovoltage (5 mV on 5 nF of a 1-mm^2 area) and a depth of 1 nm (the distance a or the size of the porphyrin cation) is 10^{-4} nm^{-3}. This density is rather small and produces a change in the electrostatic energy by Eq. **1** of only 0.004 kT. However, as pointed out before (16), this capacitor calculation seriously underestimates the charge generated inside the membrane. One can only measure potentials in the same phase so the charge near the reactive interface (actually a dipole) must polarize the opposite interface to induce a measurable potential between the two aqueous phases. In the equivalent circuit language, the charge is not on a capacitor of $\varepsilon = 3$, $l = 5$ nm (the hydrocarbon core) but on a capacitor of $\varepsilon = 25$, $l = 1$ nm (the polar region of the lipid bilayer). We refer to this as the

"chemical capacitance" (16). Thus the actual photogenerated charge is 40 times that measured, $\rho_{p+} \approx 4 \times 10^{-3}$ nm^{-3}. We reach this same conclusion by calculating the potential at the opposite interface with the electrostatic model of Fig. 1.

Using the estimated photogenerated charge, the interporphyrin cation spacing is 16 nm (i.e., the lattice is still two dimensional, $d > a, b$). The calculation of the electrostatic effect, with $a = b = 1$ nm, $\varepsilon_1 = 30 - 10$, now produces an energy of $0.16 - 0.40\ kT$, which is compatible with the data. We note that the distance a need not be the same for anions and cations in the polar region. The parameters, g^2/ε_1 and ρ_{p+}, are only estimates. A better measure of these parameters will be obtained by numerical integration of the equation for diffusion in a potential with a depth-dependent dielectric constant (32) and fitting to data of the photogating effect versus concentration of hydrophobic ions.

The magnitude of photogating is predicted to decrease with increasing concentration of $TPhP^+$, as is observed. The porphyrin cation adds to the space charge of the hydrophobic cation that, as it becomes current limiting, can only allow a yet smaller change. The increase of the photogating effect with increasing concentration of hydrophobic anions can be represented as the cancellation of discrete space charge by ion pairing. The degree of cancellation will depend on the orientation of the ion pairs. At high concentrations, where the conductance of $TPhB^-$ is saturated, the conductivity in that fraction of the area where the porphyrin cation has cancelled the space charge increases toward the zero space charge value, while the conductance in the remaining area remains at its saturated value. Thus for $\rho_- > \rho_{p+}$ the maximum conductivity G will be:

$$G \propto f_- e^{-A\rho_-} + f_{p+}, \qquad [3]$$

where f_- and f_{p+} are fractional areas occupied by the anions and the ion pairs. The normalized photogated conductivity will be:

$$G_{p+}/G_0 = f_- + f_{p+} e^{A\rho_-}, \qquad [4]$$

where G_0 is the conductance in the absence of $p+$, $f_- = 1$. The effect can be large even if f_{p+} is only 10% of f_- because of the exponential term that can easily reach values of 10^2. Using the parameters estimated above, Eq. **4** predicts conductivity increases by factors of 1.3 to 100 with increasing hydrophobic anion concentration, in agreement with observation. A more realistic estimate for Eq. **3** is that the f_{p+} term retains about one-half of the potential caused by ρ_-. We conclude that charge effects in the lipid bilayer can be accounted for by a discrete localized charge model.

As expected, experiment shows that the inner potential of the photogating effect does not detectably change (±2%) the current caused by the ion channels of amphotericin B or gramicidin A. The polar medium in the channel pore reduces the inner potential to a negligible value.

CONCLUSIONS

These results show lipophilic ion currents through a lipid bilayer membrane can be photogated by charging the membrane by photo or chemical ionization of MgOEP in the membrane. The observed photogating is qualitatively explained by space charge effects inside the bilayer membrane. The change of the inner membrane potential affects both the conductance and concentration of hydrophobic ions inside the membrane. A quantitative study of the conductance transients may determine the relative contributions of these effects. Since photocharging of the membrane occurs on the nanosecond time scale, the transients of ion transport can be examined without the problems associated with charge- and voltage-pulse methods.

The excess charge transported for the hydrophobic negative ions amounts to ≈15 nC (limited by the driving voltage and porphyrin cation lifetime) whereas the gating charge is 1 nC (estimated); therefore, the photogating effect has a net "gain" not only in current but in total transported charge. This gain is even larger (300 times) for the protonophore. Thus the photogating effect is a working example of an organic field effect phototransistor (6).

This research was supported by Grant GM25693 from the National Institutes of Health.

1. Fendler, J. H. (1984) *Annu. Rev. Phys. Chem.* **35,** 137–157.
2. Mueller, P., Rudin, D. O., Tien, H. T. & Wescott, W. C. (1963) *J. Phys. Chem.* **67,** 534–535.
3. Hille, B. (1984) *Ion Channels of Excitable Membranes* (Sinauer, Sunderland, MA).
4. Miller, C. (1986) *Ion Channel Reconstitution* (Plenum, New York).
5. Pullman, A. (1987) *Q. Rev. Biophys.* **20,** 173–200.
6. Carter, F. L. (1982) *Molecular Electronic Devices* (Dekker, New York).
7. Liberman, E. A. & Toply, V. P. (1969) *Biophysics* **14,** 477–487.
8. LeBlanc, O. H. (1969) *Biochim. Biophys. Acta* **193,** 350–360.
9. Lauger, P., Benz, R., Stark, G., Bamberg, E., Jorden, P. C., Fahr, A. & Brock, W. (1981) *Q. Rev. Biophys.* **14,** 513–583.
10. Ketterer, B., Neumke, B. & Lauger, P. (1971) *J. Membr. Biol.* **5,** 225–245.
11. Bender, C. J. (1988) *Chem. Soc. Rev.* **17,** 317–346.
12. Haydon, D. A. & Hladky, S. B. (1972) *Q. Rev. Biophys.* **5,** 187–282.
13. Parsegian, V. A. (1969) *Nature (London)* **221,** 844–846.
14. Pichar, H. & Hobbs, J. (1982) *Biochim. Biophys. Acta* **693,** 221–236.
15. Hong, F. (1976) *Photochem. Photobiol.* **24,** 155–189.
16. Hong, F. & Mauzerall, D. (1976) *J. Electrochem. Soc.* **123,** 1317–1324.
17. Woodle, M., Zhang, J. & Mauzerall, D. (1987) *Biophys. J.* **52,** 577–586.
18. Woodle, M. & Mauzerall, D. (1986) *Biophys. J.* **50,** 431–439.
19. Andersen, O. S., Feldberg, S., Nakadonari, H., Levy, S. & McLaughlin, S. (1978) *Biophys. J.* **21,** 35–70.
20. Topping, J. (1927) *Proc. R. Soc. London Ser. A* **114,** 67.
21. Harnwell, G. P. (1949) *Principles of Electricity and Electromagnetism* (McGraw–Hill, New York).
22. Flewelling, R. F. & Hubbell, W. L. (1986) *Biophys. J.* **49,** 531–552.
23. Andersen, O. S. (1978) in *Membrane Transport in Biology*, ed. Giefish, G. (Springer, New York), Vol. 1, pp. 349–446.
24. Thomas, J. K. (1980) *Chem. Rev.* **80,** 283–299.
25. Bellemare, F. & Fragata, M. (1980) *J. Colloid. Interface Sci.* **77,** 243–352.
26. Nuemcke, B. & Lauger, P. (1970) *J. Membr. Biol.* **3,** 54–66.
27. Braun, H. P. (1987) *Biochim. Biophys. Acta* **903,** 292–302.
28. de Levie, R. & Moreira, H. (1972) *J. Membr. Biol.* **9,** 241–260.
29. de Levie, R., Seidah, N. G. & Moreira, H. (1972) *J. Membr. Biol.* **10,** 171–192.
30. de Levie, R. & Seidah, N. G. (1974) *J. Membr. Biol.* **16,** 1–16.
31. de Levie, R., Seidah, N. G. & Moreira, H. (1974) *J. Membr. Biol.* **16,** 17–42.
32. Raudino, A. & Mauzerall, D. (1986) *Biophys. J.* **50,** 441–449.